

Cationic Silver Nanoclusters as Potent Antimicrobials against Multidrug-Resistant Bacteria

Zil-e Huma,[†] Akash Gupta,^{‡,§} Ibrahim Javed,^{†,§} Riddha Das,[‡] Syed Zajif Hussain,[†] Shazia Mumtaz,[†] Irshad Hussain,^{*,†} and Vincent M. Rotello^{*,‡,§}

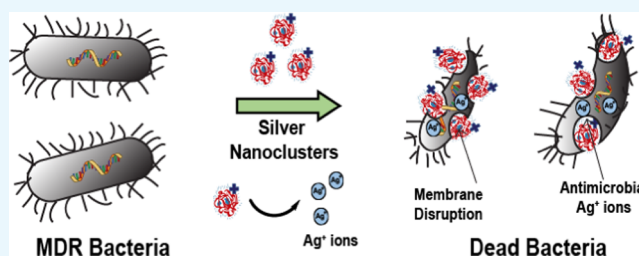
[†]Department of Chemistry & Chemical Engineering, SBA School of Science & Engineering (SBASSE), Lahore University of Management Science (LUMS), DHA, Lahore 54792, Pakistan

[‡]Department of Chemistry, University of Massachusetts (UMass) Amherst, 710 North Pleasant Street, Amherst, Massachusetts 01003, United States

[§]ARC Centre of Excellence in Convergent Bio-Nano Science and Technology, Monash Institute of Pharmaceutical Sciences, Monash University, 381 Royal Parade, Parkville, VIC 3052, Australia

S Supporting Information

ABSTRACT: Bacterial multidrug resistance (MDR) is a serious healthcare issue caused by the long-term subtherapeutic clinical treatment of infectious diseases. Nanoscale engineering of metal nanoparticles has great potential to address this issue by tuning the nano–bio interface to target bacteria. Herein, we report the use of branched polyethyleneimine-functionalized silver nanoclusters (bPEI–Ag NCs) to selectively kill MDR pathogenic bacteria by combining the antimicrobial activity of silver with the selective toxicity of bPEI toward bacteria. The minimum inhibitory concentration of bPEI–Ag NCs was determined against 12 uropathogenic MDR strains and found to be 10- to 15-fold lower than that of PEI and 2- to 3-fold lower than that of AgNO₃ alone. Cell viability and hemolysis assays demonstrated the biocompatibility of bPEI–Ag NCs with human fibroblasts and red blood cells, with selective toxicity against MDR bacteria.



INTRODUCTION

Pathogenic bacteria with acquired resistance are responsible for millions of infections and thousands of deaths worldwide.¹ In the United States alone, annually 2 million patients are victimized by hospital-acquired infections with 99 000 annual deaths, causing economic burden of \$35 billion a year.^{2,3} Significantly, ~60% of nosocomial (hospital-related) infections in the United States are caused by multidrug resistance (MDR) bacteria.^{4,5} Recently, in developing countries like Pakistan, 71% infections of newborn babies are caused by MDR bacteria. Initially, the development of new antibiotics² and antibiotic combinations was sufficient to address different pathways of resistance simultaneously.³ However, these strategies are changing the pattern of antibacterial resistance in a predictable manner, resulting in the loss of efficacy of current clinical treatments.⁶

The prominent clinical reason for the development of MDR bacterial strains is the long-term, subtherapeutic exposure of microbes to antibiotics.^{7,8} Multidrug-resistant “superbugs”, both Gram-positive (such as *Enterococcus faecium*) and Gram-negative (including *Klebsiella pneumoniae*, *Acinetobacter baumannii*, *Pseudomonas aeruginosa*, and *Enterobacter*) species, lead to serious community health hazards. However, continuous rise of multiple-antibiotic-resistant bacterial strains drives the search for new antimicrobial agents and methods to

control the growth of MDR bacterial strains. The eventual goal of these studies is to develop cost-effective, potent, safe, readily available, and easily synthesized alternatives to the conventional antibiotics that are increasingly becoming ineffective against MDR pathogens.^{9–11}

Targeting bacterial membrane using cationic, hydrophobic nanoparticles (NPs); peptidoglycan-recognizing agents; metals; and inhibitors of ATPase can provide an efficient strategy to control these superbugs.^{12–14} Nanoparticles provide an efficient platform to target MDR bacteria owing to their high surface-to-volume ratio, facile surface modification, and controllable size.^{15,16} The nature of the core material, size, and surface chemistry play significant roles in the antibacterial properties of nanoparticles. Metals, especially silver (Ag), have promising antimicrobial potential arising from dissolved Ag⁺ ions that are effective against a wide range of MDR strains.¹⁷ Decreasing the size of NPs improves their surface-to-volume ratio, leading to an enhancement in their dissolution and hence antimicrobial activity.^{18–20} Surface charge is also important, with cationic nanoparticles serving as efficient self-therapeutic antimicrobial candidates that induce cellular membrane

Received: September 19, 2018

Accepted: November 21, 2018

Published: December 5, 2018

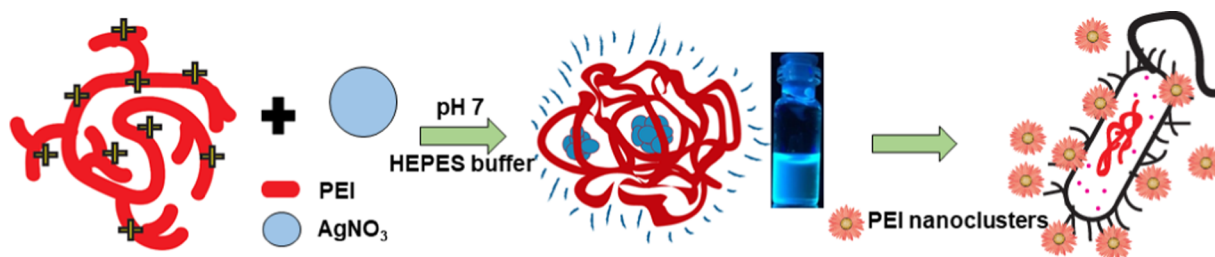


Figure 1. General scheme for the synthesis of bPEI-coated Ag NCs (bPEI–Ag NCs) and their antibacterial action.

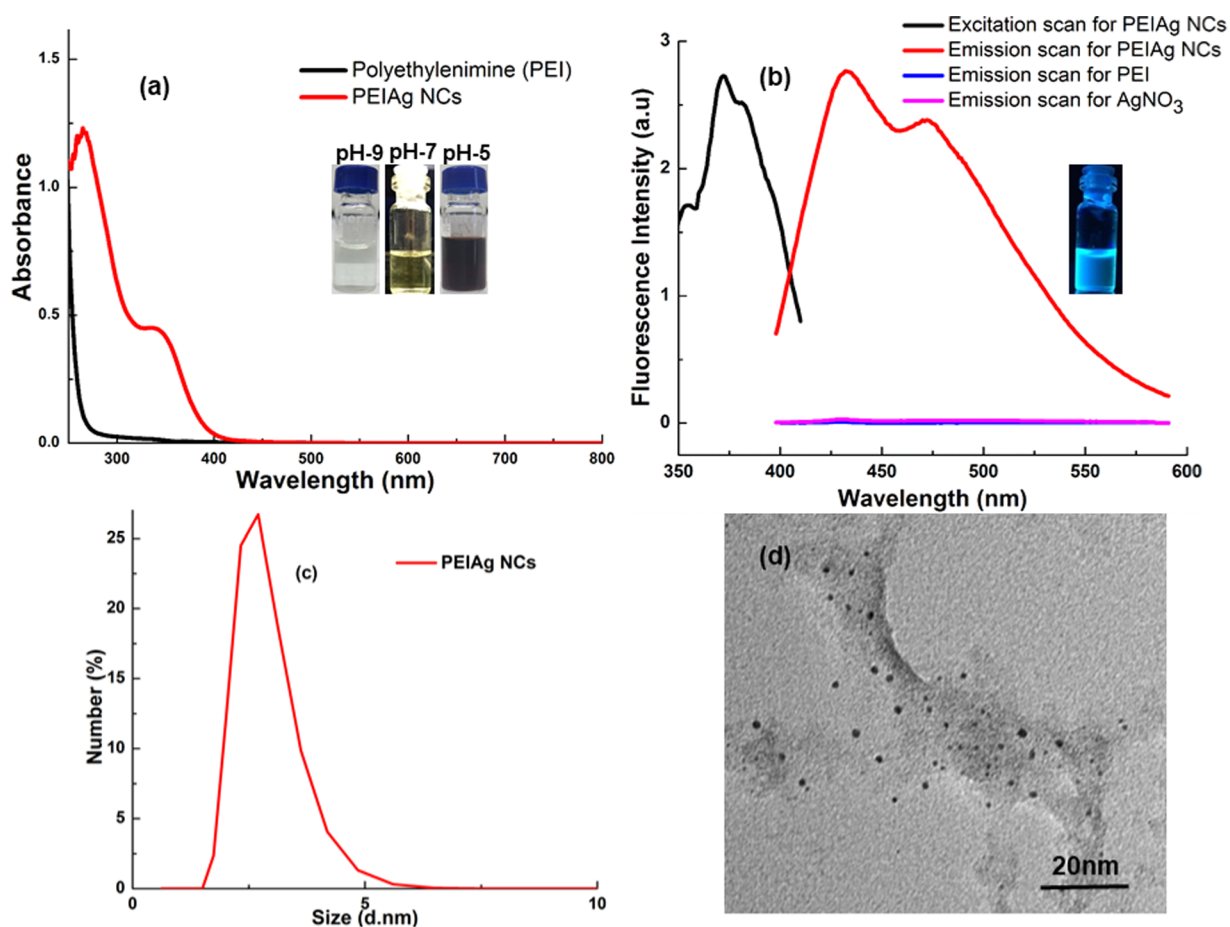


Figure 2. (a) UV–visible absorption spectrum of polyethylenimine silver nanoclusters (bPEI–Ag NCs) and polyethylenimine (PEI) showing multiple absorption peaks for Ag nanoclusters compared to those for PEI, and the inset shows bPEI–Ag NCs in 4-(2-hydroxyethyl)piperazine-1-ethanesulfonic acid (HEPES) buffer (pH 7.0–9.0). (b) Photoluminescence spectrum of blue fluorescent bPEI–Ag NCs showing excitation at 375 nm and emission at 430 nm. (c) Dynamic light scattering (DLS) analysis showing an average hydrodynamic diameter of 3 nm. (d) TEM micrographs of bPEI–Ag NCs.

disruption.^{21,22} This ability to lyse bacteria with reduced mammalian cell toxicity involves the adjustment in the proportion of surface charge and hydrophobicity.^{12,21,23} Increasing the biocompatibility of cationic antimicrobial agents through a rational design by encapsulating bioactive molecules using biocompatible polymers²⁴ like polyamidoamine,²⁵ chitosan, and branched polyethylenimine (bPEI)²⁶ is an attractive research direction in this regard.^{27,28}

Combinations of antimicrobials can synergistically increase the therapeutic efficacy.²⁹ We therefore set out to use a combination of PEI and silver in the form of silver nanoclusters (Ag NCs) to target MDR bacteria.³⁰ In this work, we synthesized blue fluorescent cationic silver nanoclusters coated with low molecular weight bPEI (bPEI–Ag NCs) and

characterized these polymer-coated nanoclusters using optical measurements and electron microscopic techniques. The prepared nanoclusters demonstrated pronounced antibacterial activity against 12 multidrug uropathogenic (pathogens associated with urinary tract infections) strains of bacteria. Scanning electron microscopy (SEM) imaging and the live/dead bacterial staining assay showed that bPEI–Ag NCs target bacteria through the membrane disruption mechanism. Significantly, these nanoclusters exhibited minimal hemolysis toward red blood cells and low toxicity against mammalian cells, making them promising therapeutics for bacterial infections.

Table 1. MIC Data of Polyethylenimine Silver Nanoclusters (bPEI–Ag NCs)

sr. no.	strain name	pathogenicity	species	no. of resistant drugs	MIC of Ag NCs (nM)	MIC of AgNO ₃ (nM)	MIC of PEI (nM)	MDR
1	ATCC 19660	nonpathogenic	<i>P. aeruginosa</i>	0	0.03	0.125	>32	no
2	CD-549	uropathogenic	<i>Escherichia coli</i>	16	0.06	0.125	>32	yes
3	CD-1006	uropathogenic	<i>P. aeruginosa</i>	1	0.125	0.5	>32	no
4	CD-2	uropathogenic	<i>E. coli</i>	1	0.25	2	>32	no
5	CD-489	uropathogenic	<i>Staphylococcus aureus</i> MRSA	10	0.015	0.03	>32	yes
6	CD-23	uropathogenic	<i>P. aeruginosa</i>	13	0.125	0.5	>32	yes
7	N/A	nonpathogenic	<i>A. azurea</i>		0.125	0.25	>32	
8	CD-3	uropathogenic	<i>E. coli</i>	3	0.06	0.25	>32	yes
9	CD-1412	uropathogenic	<i>Enterobacter cloacae</i> complex	4	0.06	0.25	>32	yes
10	CD-746	uropathogenic	<i>Enterococcus faecalis</i>		0.25	0.5	>32	no
11	CD-866	uropathogenic	<i>E. cloacae</i> complex	2	0.25	1	>32	yes
12	CD-895	uropathogenic	<i>E. faecalis</i>	2	0.06	0.125	>32	yes
13	CD-1578	uropathogenic	<i>Staphylococcus aureus</i>	4	0.06	0.5	>32	yes
14	CD-14	uropathogenic	<i>P. aeruginosa</i>	7	0.06	0.25	>32	yes

RESULTS AND DISCUSSION

The bPEI–Ag NCs were synthesized through a one-pot, single-step reaction (Figure 1) and were further characterized for their absorption and photoluminescence properties, sizes, and morphologies.

The solutions of bPEI–Ag NCs were light yellow under visible light and displayed blue fluorescence under UV illumination at 365 nm. The absorption spectrum showed two absorption bands at 268 and 354 nm (Figure 2a). The absorption peak at 354 nm corresponds to the oligomeric silver species. The absence of the surface plasmon resonance band of larger Ag NPs between 400 and 500 nm indicates the formation of smaller Ag nanoclusters.³¹ The maximum fluorescence emission of bPEI–Ag NCs was 430 nm at an excitation wavelength of 365 nm, which confirms the synthesis of silver nanoclusters (Figure 2b).³² The hydrodynamic size of these nanoclusters was found to be ~3 nm (Figure 2c) with a ζ -potential of +30 mV (Figure S1). High-resolution transmission electron microscopy (HRTEM) analysis revealed isotropic and spherical morphology of Ag NCs with an average core diameter of ~2 nm (Figure 2d). The amount of elemental silver in the bPEI–Ag NC solution was determined to be 8.95 $\mu\text{g}/\text{mL}$ (Supporting Information) using inductively coupled plasma mass spectrometry.³³ This estimation will be helpful to target concentrations of controls to make the antibacterial assay more reproducible.

The antibacterial activity of cationic bPEI–Ag NCs was explored against lab strains of *P. aeruginosa* (ATCC 19660, Gram-negative) and *Amycolatopsis azurea* (Gram-positive) and 12 uropathogenic clinical MDR isolates (Table 1). The minimum inhibitory concentration (MIC) of bPEI was 32 nM, whereas that of AgNO₃ was around 2–0.125 nM against different lab strains. The MIC of bPEI-coated Ag NCs was, however, found to be 2- to 3-fold better than that of AgNO₃ alone (Figure S2). bPEI–Ag NCs could selectively suppress the growth of these pathogens, with MICs ranging from 0.25 to 0.015 nM. Functionalized bPEI–Ag NCs could inhibit the growth of resistant superbug methicillin-resistant *Staphylococcus aureus* (MRSA) at a concentration as low as 0.015 nM. Similar MIC values for clinical MDR and lab strains suggest that bPEI–Ag NCs could possibly share the common mechanism of targeting bacterial resistance.^{34,35} The antibacterial activity of bPEI–Ag NCs can be attributed to the

cationic nature of surface ligands composed of hydrophobic segments that facilitate the contact of bPEI–Ag NCs with bacterial cells that causes membrane damage, as well as the release of Ag⁺ ions from the bPEI–Ag NCs. The increased surface area of the bPEI–Ag NCs could increase the sustained dissolution of the Ag⁺; a process distinctively different from a burst release of Ag⁺ ions when directly used in the form of AgNO₃.³⁶ The bactericidal activity of PEI due to its cationic nature adds to the bactericidal activity along with Ag⁺, resulting in the observed broad-spectrum antibacterial activity of bPEI–Ag NCs.^{37,38}

The selectivity of antimicrobial agents to bacteria as opposed to mammalian cells is essential for their therapeutic efficacy.³⁹ bPEI–Ag NCs showed low dose-dependent cytotoxicity against fibroblasts. IC₅₀ for bPEI–Ag NCs against fibroblasts was 38 nM (Figure 3), indicating their safe therapeutic window.

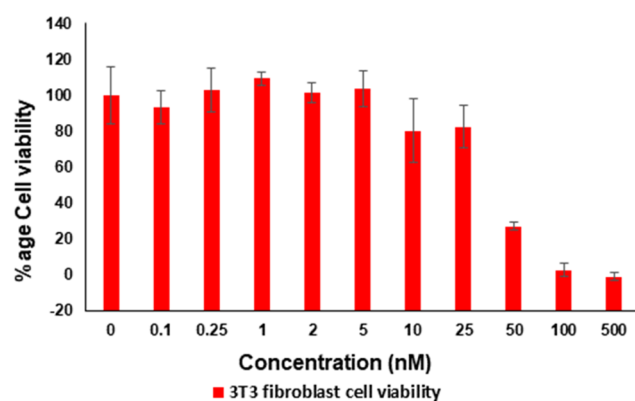


Figure 3. Cell viability test of polyethylenimine silver nanoclusters (bPEI–Ag NCs) to test their cytotoxicity against fibroblasts.

Hemolysis assays were performed to examine the biocompatibility of bPEI–Ag NCs with human red blood cells, as RBCs are highly susceptible to lysis upon systemic administration of nanomedicine.³³ In the complete range of MIC concentrations of bPEI–Ag NCs against bacteria (0.25–0.015 nM) (Figure S3), silver nanoclusters showed minimal hemolytic activity. HC₅₀, the concentration of Ag NCs required to lyse 50% of RBCs, was much higher than ~500

nM, with the resulting therapeutic index (HC_{50}/MIC) > 2000 (500/0.25). This indicates that these Ag NCs can be injected safely through blood without causing hemolysis of the RBCs. Previous studies on hemolysis by PEI and silver ions indicate that the polymer shows high hemolytic activity at therapeutically relevant concentrations, whereas bPEI–Ag NCs show minimal hemolytic activity, as shown in Figure 4, further

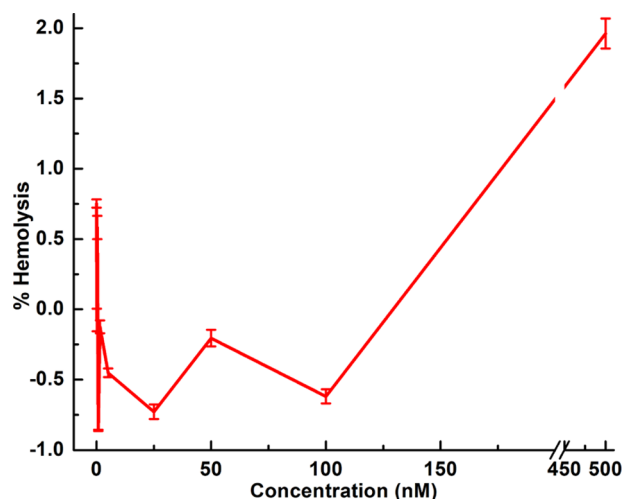


Figure 4. Hemolysis study of polyethyleneimine silver nanoclusters (bPEI–Ag NCs) to test their compatibility with red blood cells.

corroborating the biocompatibility of Ag NCs.⁴⁰ The observed high selectivity of bPEI–Ag NCs against bacterial cells may be attributed to the bacteria having more negatively charged surface than that of the mammalian cells. Moreover, mammalian cell membranes are highly stabilized because of the presence of cholesterol that makes them less vulnerable to antimicrobial metal NCs.^{41,42}

After establishing the biocompatibility of Ag NCs with RBCs and mammalian cells, we further probed the bactericidal nature of Ag NCs using the live/dead assay. In this experiment, *E. coli* cells (1×10^8 cfu/mL) were incubated with bPEI–Ag NCs to a final concentration of 40 nM for 2 h at 37 °C, followed by staining with live/dead assay reagents. Confocal laser microscopic images (Figure 5) showed bacterial cells with compromised membranes of dead bacterium. Calcein acetoxymethyl ester crosses the intact membranes of live cells and is converted into calcein, a green fluorescent molecule, inside the viable cells as in (a), whereas propidium iodide (PI) can only

enter the cells with compromised membranes, resulting in red fluorescence. The strong red fluorescence of cells (b) treated with bPEI–Ag NCs indicated compromised bacterial membranes. The simultaneous monitoring of viable and dead cells is shown in Figure 5c.

Next, we studied the interaction of bPEI–Ag NCs with the bacterial membrane; the morphology of Ag NC-treated bacteria was studied using TEM. Microscopic observation of *E. coli* cells treated with bPEI–Ag NCs clearly revealed their abnormal morphology, whereas untreated bacterial cells as control appeared normal (Figure 6a). bPEI–Ag NC-treated cells appeared to be stressed, and membrane distortion was observed. The probable mechanism for the interaction/penetration of bPEI–Ag NCs through the bacterial membrane is the formation of breaks called pits.³⁰ The pit formation has been observed for *E. coli* using scanning TEM (STEM) (Figure 6b).^{43,36} The morphology was completely changed with total loss of integrity after 8 h (Figure 6c).⁴⁴ These Ag NCs act by forming a direct contact with the bacterial membrane, without penetrating deep into their cells, resulting in the failure of antibiotic resistance of bacteria, and are thus potential candidates to address serious global healthcare challenges like MDR because they might be less prone to resistance than antibiotics.⁴⁵

CONCLUSIONS

In summary, branched polyethyleneimine silver nanoclusters were synthesized by a chemical reduction method and are found to be potential candidates to target MDR in various pathogenic and nonpathogenic strains of bacteria. They showed multiple-fold improved bactericidal effects compared to those of controls, which is attributed to their smaller size, surface chemistry, and cationic nature. The bPEI–Ag NCs act as broad-spectrum antibiotics by targeting bacteria using the membrane disruption mechanism with limited toxicity against mammalian and red blood cells. They have broader implications of crafting nanocapsules to carry and deliver drugs against multidrug-resistant bacterial infections, in vivo, because of the combinatorial effect. These bioinorganic bPEI–Ag NCs, therefore, have the potential to provide therapeutics for antibiotic-resistant pathogens.

EXPERIMENTAL SECTION

Materials and Methods. *Chemicals.* Hyperbranched polyethyleneimine (bPEI) (M_n 800, 99%), silver nitrate, 4-(2-hydroxyethyl)piperazine-1-ethanesulfonic acid (HEPES),

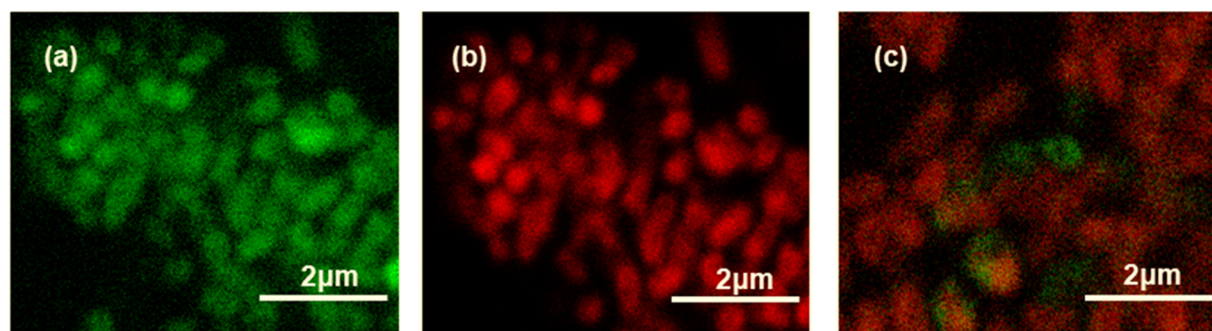


Figure 5. Confocal microscopy images of *E. coli* incubated with calcein acetoxymethyl ester and propidium iodide (PI). (a) *E. coli* as control: viable cells emit green fluorescence at 490 nm λ_{ex} and 515 nm λ_{em} . (b) *E. coli* incubated for 2 h with polyethyleneimine silver nanoclusters (bPEI–Ag NCs): dead cells emit red fluorescence at 535 nm λ_{ex} and 617 nm λ_{em} . (c) Merged image of viable and dead cells.

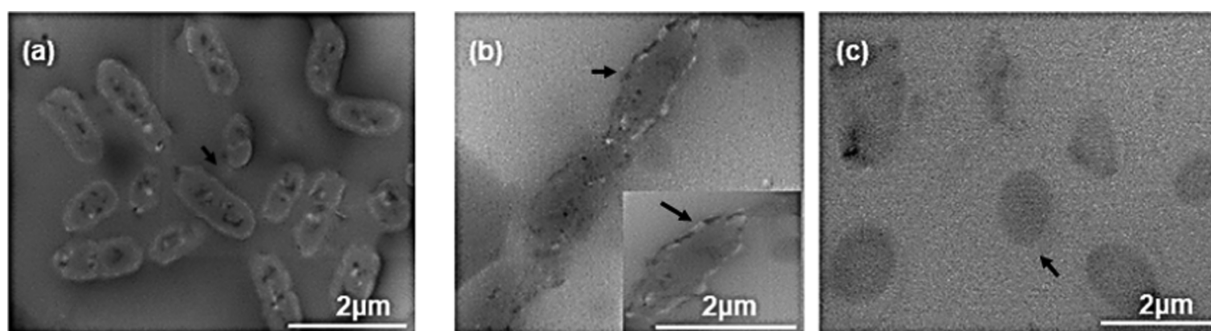


Figure 6. SEM micrographs showing interaction of *E. coli* with bPEI-AgNCs at: (a) 0 h-control, (b) 4 h incubation, and (c) 8 h incubation.

formaldehyde (30 wt %), phosphate-buffered saline (PBS 7.4 pH), and dialysis membranes (molecular weight cut-off (MWCO) 1 kD) were purchased from Sigma-Aldrich. All of the solvents used in this study were of analytical grade. Millipore water with a resistivity of 18.2 MΩ was used to prepare all of the aqueous formulations. All bacterial strains were harvested in the Cooley Dickinson Hospital Microbiology Laboratory (Northampton, MA). NIH 3T3 cells (ATCC CRL-1658) and Dulbecco's modified Eagle's medium (DMEM) (DMEM; ATCC30-2002) were purchased from ATCC, and fetal bovine serum (SH3007103) was purchased from Fisher Scientific.

Characterization. A UV-visible spectrophotometer (Shimadzu; UV-1800) was used to measure UV-visible absorption spectra of bPEI-Ag NCs in 200–800 nm range. Fluorescence measurements of bPEI-Ag NCs were carried out using a fluorescence spectrophotometer coupled with a multiplate reader (PerkinElmer; Enspire 2300). Transmission electron microscopic analysis was performed using a JEOL 7C transmission electron microscope operating at 80 keV. The sample for TEM was prepared by slowly evaporating a dilute drop of clean bPEI-Ag NCs onto a 200-mesh carbon-coated copper grid. The interaction of bacteria with Ag NCs at different time intervals was studied using a field-emission scanning electron microscope (FEI; Nova Nano SEM-450) equipped with a STEM detector operating at 10 kV. The samples for SEM were prepared by placing a drop of a dilute solution of bPEI-Ag NCs, incubated with bacteria, on carbon-coated copper grids, followed by air-drying. The bacteria on copper grids were then fixed using 2.5% solution of glutaraldehyde (prepared in normal saline), followed by subsequent dehydration using a series of acetone dilutions, i.e., 30, 50, 70, 80, 90, and 100% for 10 min each.⁴⁶ The dynamic light scattering (DLS) measurements of bPEI-Ag NCs were performed using a Zetasizer system (Malvern, Nano ZSP).

Synthesis of Polyethylenimine Silver Nanoclusters (bPEI-Ag NCs). bPEI-Ag NCs were prepared using a modified silver mirror reaction. Briefly, 1 mL aqueous solution of PEI (0.094 g), 50 μL of HEPES (1 M), and 950 μL of H₂O were vigorously stirred for 2 min followed by a dropwise addition of 2.5 mL of AgNO₃ (0.01 M). Silver ions were first sequestered in bPEI forming a bPEI-Ag complex, which is resistant against reduction under basic conditions (pH 9.0) even with NaBH₄. The pH was adjusted to 7 with the HEPES buffer, resulting in a change of solution color from colorless to light yellow because of the formation of a complex. At neutral pH, the reduction potential for the Ag⁺/Ag system is 0.799 V, whereas that for Ag(NH₃)⁺/Ag is 0.379 V.^{26,47,32} Formaldehyde (100

μL) (30%) was then slowly added, and the reaction mixture was stirred for 10 min at 70 °C. PEI can etch the larger Ag NPs to smaller Ag NCs; hence, upon prolonged incubation of the reaction mixture (24 h), polyethylenimine silver nanoclusters (bPEI-Ag NCs) were obtained.⁴⁸ The bPEI-Ag NCs were purified by dialysis in deionized water using a 1 kD (MWCO) membrane for 24 h and stored in the dark at 4 °C for further use. UV-vis absorption spectra of bPEI-Ag NCs show absorption peaks at 268 and 354 nm, which correspond to Ag NCs; however, pure PEI shows only one absorption peak at 260 nm, which overlaps with that of the absorption of glass cell. The Ag NCs were synthesized at 70 °C, and the absorption peaks at 268 and 354 nm due to Ag NCs were disappeared upon further increasing the temperature and a new absorption peak emerged at 400 nm (surface plasmon resonance), which corresponds to silver nanoparticles. The complete wavelength scan showed that the corresponding excitation and emission wavelengths for bPEI-Ag NCs were 375 and 430 nm, respectively. Pure PEI also displayed similar excitation and emission peaks, but the fluorescence intensities were about 1/60th of those exhibited by bPEI-Ag NCs.

In Vitro Studies. The antibacterial activity of bPEI-Ag NCs was measured as the minimum inhibitory concentration (MIC) through the broth dilution method. MIC is the minimum concentration of the chemical required to prevent visible growth of bacterium. For this purpose, different bacterial strains (Table 1) were grown overnight in the lysogeny broth and their optical density (OD) was measured at 600 nm after washing them with PBS to separate viable bacteria. bPEI-Ag NC solutions of eight different concentrations in the range of (16–0.03 nM) were prepared by serial dilution. The Ag NCs were incubated with 5 × 10⁵ cfu/mL bacteria for 16 h in an incubator at 37 °C and 275 rpm. The media and bacteria without bPEI-Ag NCs were employed as negative and positive controls, respectively. Finally, after 16 h, the OD was measured again at 600 nm to check the concentration of living bacteria.^{12,49}

Cell Viability Assay. A total of 20 000 NIH 3T3 (ATCC CRL-1658) fibroblasts were cultured in Dulbecco's modified Eagle medium (DMEM) with 10% bovine calf serum (BSA) and 1% antibiotics at 37 °C in a humidified atmosphere of 5% CO₂ for 48 h. Old media was removed, and cells were washed with phosphate-buffered saline (PBS) before the addition of bPEI-Ag NCs in prewarmed 10% BSA in media. The silver nanoclusters and cells were then incubated for 24 h at 37 °C under a humidified atmosphere of 5% CO₂. Cell viability was determined using the alamar blue assay following the manufacturer's protocol.⁵⁰ Briefly, cells washed with PBS were treated with 220 μL of 10% alamar blue in BSA serum

containing media and incubated at 37 °C under a humidified atmosphere of 5% CO₂ for 3 h. After incubation, 200 μL of solution from each well was transferred into a 96-well black microplate. Red epifluorescence intensity, resulting from the alamar blue solution, was measured (excitation/emission: 560/590 nm) using a Spectro Max M5 microplate reader (Molecular Devices) to determine the cellular viability. Cells without bPEI–Ag NCs were considered as 100% viable. Each experiment was performed in triplicate.

Hemolysis Assay. Citrate-stabilized human whole blood (pooled, mixed gender) was purchased from Bioreclamation LLC, NY, and immediately processed. For this purpose, 10 mL of phosphate-buffered saline (PBS) was added to the blood (2 mL) and centrifuged at 5000 rpm for 5 min. The supernatant was carefully discarded, the red blood cells (RBCs) were dispersed in 10 mL of PBS, and the solution was kept on ice during the procedure. The RBC solution (0.1 mL) was added to 0.4 mL of the bPEI–Ag NC solution in PBS in a 1.5 mL centrifuge tube (Fisher) and mixed gently by pipetting. RBCs incubated with PBS and water were used as negative and positive controls, respectively. All bPEI–Ag NC samples as well as controls were prepared in triplicate. The mixture was incubated at 37 °C for 30 min with gentle shaking at 150 rpm. After incubation, the solution was centrifuged at 4000 rpm for 5 min and 100 μL of the supernatant was transferred to a 96-well plate. The absorbance of the supernatant was measured at 570 nm using a microplate reader (Spectra Max M2, Molecular Devices) with absorbance at 655 nm as a reference.⁴⁴

■ ASSOCIATED CONTENT

📄 Supporting Information

The Supporting Information is available free of charge on the ACS Publications website at DOI: [10.1021/acsomega.8b02438](https://doi.org/10.1021/acsomega.8b02438).

Calculation of concentration of Ag in bPEI–Ag NCs; ζ-potential of polyethylenimine silver nanoclusters (bPEI–Ag NCs); minimum inhibitory concentration of polyethylenimine, silver nitrate, and polyethylenimine silver nanoclusters (bPEI–Ag NCs) against different bacterial lab strains; hemolysis study of polyethylenimine silver nanoclusters (bPEI–Ag NCs) to test their toxicity against RBCs (PDF)

■ AUTHOR INFORMATION

Corresponding Authors

*E-mail: ihussain@lums.edu.pk (I.H.).

*E-mail: rotello@chem.umass.edu (V.M.R.).

ORCID

Akash Gupta: 0000-0001-5614-2313

Ibrahim Javed: 0000-0003-1101-5614

Syed Zajif Hussain: 0000-0002-3834-6061

Irshad Hussain: 0000-0001-5498-1236

Vincent M. Rotello: 0000-0002-5184-5439

Notes

The authors declare no competing financial interest.

■ ACKNOWLEDGMENTS

V.M.R. acknowledges support from the National Institutes of Health (R01 AI134770). Clinical samples were kindly provided by Dr Margaret Riley through the Cooley Dickinson Hospital Microbiology Laboratory (Northampton, MA).

V.M.R. and I.H. acknowledge the partial support from the US National Academy of Sciences and Pakistan Higher Education Commission (HEC).

■ ACRONYMS

NPs, nanoparticles
PEI, polyethylenimine
NCs, nanoclusters
MIC, minimum inhibitory concentration
MDR, multidrug resistance
HEPES, 4-(2-hydroxyethyl)piperazine-1-ethanesulfonic acid

■ REFERENCES

- (1) Levy, S. B.; Marshall, B. Antibacterial resistance worldwide: causes, challenges and responses. *Nat. Med.* **2004**, *10*, S122–S129.
- (2) Lin, G.; Mi, P.; Chu, C.; Zhang, J.; Liu, G. Inorganic nanocarriers overcoming multidrug resistance for cancer theranostics. *Adv. Sci.* **2016**, *3*, No. 1600134.
- (3) Wenzel, R. P.; Edmond, M. B. Managing antibiotic resistance. *N. Engl. J. Med.* **2000**, *343*, 1961–1963.
- (4) Norman, R. S.; Stone, J. W.; Gole, A.; Murphy, C. J.; Sabo-Attwood, T. L. Targeted photothermal lysis of the pathogenic bacteria, *Pseudomonas aeruginosa*, with gold nanorods. *Nano Lett.* **2008**, *8*, 302–306.
- (5) Ayala-Núñez, N. V.; Villegas, H. H. L.; et al. Silver nanoparticles toxicity and bactericidal effect against methicillin-resistant *Staphylococcus aureus*: nanoscale does matter. *Nanobiotechnology* **2009**, *5*, 2–9.
- (6) Fischbach, M. A. Combination therapies for combating antimicrobial resistance. *Curr. Opin. Microbiol.* **2011**, *14*, 519–23.
- (7) Agarwal, V.; Nair, S. K. *Infectious Disease Diagnosis*; Springer, 2013; pp 7–26.
- (8) Christena, L. R.; Mangalagowri, V.; Pradheeba, P.; Ahmed, K. B. A.; Shalini, B. I. S.; Vidyalakshmi, M.; Anbazhagan, V.; Subramanian, N. S. Copper nanoparticles as an efflux pump inhibitor to tackle drug resistant bacteria. *RSC Adv.* **2015**, *5*, 12899–12909.
- (9) Eby, D. M.; Schaeublin, N. M.; Farrington, K. E.; Hussain, S. M.; Johnson, G. R. Lysozyme catalyzes the formation of antimicrobial silver nanoparticles. *ACS Nano* **2009**, *3*, 984–994.
- (10) Zhao, Y.; Tian, Y.; Cui, Y.; Liu, W.; Ma, W.; Jiang, X. Small molecule-capped gold nanoparticles as potent antibacterial agents that target Gram-negative bacteria. *J. Am. Chem. Soc.* **2010**, *132*, 12349–12356.
- (11) Landis, R. F.; Li, C. H.; Gupta, A.; Lee, Y. W.; Yazdani, M.; Ngernyung, N.; Altinbasak, I.; Mansoor, S.; Khichi, M. A. S.; Sanyal, A.; et al. Biodegradable Nanocomposite Antimicrobials for the Eradication of Multidrug-Resistant Bacterial Biofilms without Accumulated Resistance. *J. Am. Chem. Soc.* **2018**, *140*, 6176–6182.
- (12) Gupta, A.; Saleh, N. M.; Das, R.; Landis, R. F.; Bigdeli, A.; Motamedchaboki, K.; Rosa Campos, A.; Pomeroy, K.; Mahmoudi, M.; Rotello, V. M. Synergistic Antimicrobial Therapy Using Nanoparticles and Antibiotics for the Treatment of Multidrug-Resistant Bacterial Infection. *Nano Futures* **2017**, *1*, No. 015004.
- (13) Zhao, Y.; Chen, Z.; Chen, Y.; Xu, J.; Li, J.; Jiang, X. Synergy of non-antibiotic drugs and pyrimidinethiol on gold nanoparticles against superbugs. *J. Am. Chem. Soc.* **2013**, *135*, 12940–12943.
- (14) Yang, X.; Yang, J.; Wang, L.; Ran, B.; Jia, Y.; Zhang, L.; Yang, G.; Shao, H.; Jiang, X. Pharmaceutical intermediate-modified gold nanoparticles: against multidrug-resistant bacteria and wound-healing application via an electrospun scaffold. *ACS Nano* **2017**, *11*, 5737–5745.
- (15) Gupta, A.; Landis, R. F.; Rotello, V. M. Nanoparticle-based antimicrobials: surface functionality is critical. *F1000Research* **2016**, *5*, 1–10.
- (16) Moyano, D. F.; Saha, K.; Prakash, G.; Yan, B.; Kong, H.; Yazdani, M.; Rotello, V. M. Fabrication of corona-free nanoparticles with tunable hydrophobicity. *ACS Nano* **2014**, *8*, 6748–6755.

- (17) Rai, M. K.; Deshmukh, S.; Ingle, A.; Gade, A. Silver nanoparticles: the powerful nanoweapon against multidrug-resistant bacteria. *J. Appl. Microbiol.* **2012**, *112*, 841–852.
- (18) Baker, C.; Pradhan, A.; Pakstis, L.; Pochan, D. J.; Shah, S. I. Synthesis and antibacterial properties of silver nanoparticles. *J. Nanosci. Nanotechnol.* **2005**, *5*, 244–249.
- (19) Zheng, K.; Setyawati, M. I.; Lim, T.; Leong, D. T.; Xie, J. Antimicrobial cluster bombs: silver nanoclusters packed with daptomycin. *ACS Nano* **2016**, *10*, 7934–7942.
- (20) Lemire, J. A.; Harrison, J. J.; Turner, R. J. Antimicrobial activity of metals: mechanisms, molecular targets and applications. *Nat. Rev. Microbiol.* **2013**, *11*, 371–384.
- (21) Gupta, A.; Landis, R. F.; Li, C.-H.; Schnurr, M.; Das, R.; Lee, Y.-W.; Yazdani, M.; Liu, Y.; Kozlova, A.; Rotello, V. M. Engineered Polymer Nanoparticles with Unprecedented Antimicrobial Efficacy and Therapeutic Indices against Multidrug-Resistant Bacteria and Biofilms. *J. Am. Chem. Soc.* **2018**, 12137.
- (22) Goodman, C. M.; McCusker, C. D.; Yilmaz, T.; Rotello, V. M. Toxicity of Gold Nanoparticles Functionalized with Cationic and Anionic Side Chains. *Bioconjugate Chem.* **2004**, *15*, 897–900.
- (23) Hayden, S. C.; Zhao, G.; Saha, K.; Phillips, R. L.; Li, X.; Miranda, O. R.; Rotello, V. M.; El-Sayed, M. A.; Schmidt-Krey, I.; Bunz, U. H. F. Aggregation and Interaction of Cationic Nanoparticles on Bacterial Surfaces. *J. Am. Chem. Soc.* **2012**, *134*, 6920–6923.
- (24) Arbab, A. S.; Wilson, L. B.; Ashari, P.; Jordan, E. K.; Lewis, B. K.; Frank, J. A. A model of lysosomal metabolism of dextran coated superparamagnetic iron oxide (SPIO) nanoparticles: implications for cellular magnetic resonance imaging. *NMR Biomed.* **2005**, *18*, 383–389.
- (25) Shang, L.; Dong, S. Facile preparation of water-soluble fluorescent silver nanoclusters using a polyelectrolyte template. *Chem. Commun.* **2008**, 1088–1090.
- (26) Yuan, Z.; Cai, N.; Du, Y.; He, Y.; Yeung, E. S. Sensitive and selective detection of copper ions with highly stable polyethylenimine-protected silver nanoclusters. *Anal. Chem.* **2014**, *86*, 419–426.
- (27) Eissa, A. M.; Abdulkarim, A.; Sharples, G. J.; Cameron, N. R. Glycosylated nanoparticles as efficient antimicrobial delivery agents. *Biomacromolecules* **2016**, *17*, 2672–2679.
- (28) Qu, F.; Li, N. B.; Luo, H. Q. Highly sensitive fluorescent and colorimetric pH sensor based on polyethylenimine-capped silver nanoclusters. *Langmuir* **2013**, *29*, 1199–1205.
- (29) Worthington, R. J.; Melander, C. Combination approaches to combat multi-drug resistant bacteria. *Trends Biotechnol.* **2013**, *31*, 177–184.
- (30) Dai, X.; Guo, Q.; Zhao, Y.; Zhang, P.; Zhang, T.; Zhang, X.; Li, C. Functional silver nanoparticle as a benign antimicrobial agent that eradicates antibiotic-resistant bacteria and promotes wound healing. *ACS Appl. Mater. Interfaces* **2016**, *8*, 25798–25807.
- (31) Pauksch, L.; Hartmann, S.; Rohnke, M.; Szalay, G.; Alt, V.; Schnettler, R.; Lips, K. S. Biocompatibility of silver nanoparticles and silver ions in primary human mesenchymal stem cells and osteoblasts. *Acta Biomater.* **2014**, *10*, 439–449.
- (32) Kalishwaralal, K.; BarathManiKanth, S.; Pandian, S. R. K.; Deepak, V.; Gurunathan, S. Silver nanoparticles impede the biofilm formation by *Pseudomonas aeruginosa* and *Staphylococcus epidermidis*. *Colloids Surf., B* **2010**, *79*, 340–344.
- (33) Li, X.; Robinson, S. M.; Gupta, A.; Saha, K.; Jiang, Z.; Moyano, D. F.; Sahar, A.; Riley, M. A.; Rotello, V. M. Functional gold nanoparticles as potent antimicrobial agents against multi-drug-resistant bacteria. *ACS Nano* **2014**, *8*, 10682–10686.
- (34) Padmos, J. D.; Boudreau, R. T. M.; Weaver, D. F.; Zhang, P. Structure of tiopronin-protected silver nanoclusters in a one-dimensional assembly. *J. Phys. Chem. C* **2015**, *119*, 24627–24635.
- (35) Beyth, N.; Hourri-Haddad, Y.; Domb, A.; Khan, W.; Hazan, R. Alternative antimicrobial approach: nano-antimicrobial materials. *J. Evidence-Based Complementary Altern. Med.* **2015**, *2015*, No. 246012.
- (36) Eckhardt, S.; Brunetto, P. S.; Gagnon, J.; Priebe, M.; Giese, B.; Fromm, K. M. Nanobio silver: Its interactions with peptides and bacteria, and its uses in medicine. *Chem. Rev.* **2013**, *113*, 4708–4754.
- (37) Sangsuwan, A.; Kawasaki, H.; Matsumura, Y.; Iwasaki, Y. Antimicrobial Silver Nanoclusters Bearing Biocompatible Phosphorylcholine-Based Zwitterionic Protection. *Bioconjugate Chem.* **2016**, *27*, 2527–2533.
- (38) Godbey, W. T.; Wu, K.; Hirasaki, G.; Mikos, A. Improved packing of poly(ethylenimine)/DNA complexes increases transfection efficiency. *Gene Ther.* **1999**, *6*, 1380–1388.
- (39) Hou, Z.; Shankar, Y. V.; Liu, Y.; Ding, F.; Subramanion, J. L.; Ravikumar, V.; Zamudio, R.; Keogh, D.; Lim, K.; et al. Nanoparticles of short cationic peptidopolysaccharide self-assembled by hydrogen bonding with antibacterial effect against multidrug-resistant bacteria. *ACS Appl. Mater. Interfaces* **2017**, *9*, 38288–38303.
- (40) You, F.; Tang, W.; Yung, L. L. Real-time monitoring of Trojan-horse effect of silver nanoparticles by a genetically encoded fluorescent cell sensor. *Nanoscale* **2018**, *10*, 7726–7735.
- (41) Rajchakit, U.; Sarojini, V. Recent developments in antimicrobial-peptide-conjugated gold nanoparticles. *Bioconjugate Chem.* **2017**, *28*, 2673–2686.
- (42) Sadamoto, R.; Niikura, K.; Sears, P. S.; Liu, H.; Wong, C.; Suksumcheep, A.; et al. Cell wall engineering of living bacteria. *J. Am. Chem. Soc.* **2002**, *124*, 9018–9019.
- (43) Kim, H.; Namgung, R.; Singha, K.; Oh, I. K.; Kim, W. J. Graphene oxide-polyethylenimine nanoconstruct as a gene delivery vector and bioimaging tool. *Bioconjugate Chem.* **2011**, *22*, 2558–2567.
- (44) Khan, Z.; Rehman, A.; Nisar, M. A.; Zafar, S.; et al. Molecular basis of Cd²⁺ stress response in *Candida tropicalis*. *Appl. Microbiol. Biotechnol.* **2017**, *101*, 7715–7728.
- (45) Wiegand, I.; Hilpert, K.; Hancock, R. E. Agar and broth dilution methods to determine minimum inhibitory concentration (MIC) of antimicrobial substances. *Nat. Protoc.* **2008**, *3*, 163–175.
- (46) Kim, K.; Lee, H. B.; Lee, J. W.; Park, H. K.; Shin, K. S. Self-Assembly of poly(ethylenimine)-capped Au nanoparticles at a toluene–water interface for efficient surface-enhanced Raman scattering. *Langmuir* **2008**, *24*, 7178–7183.
- (47) Qu, F.; Li, N. B.; Luo, H. Q. Transition from nanoparticles to nanoclusters: microscopic and spectroscopic investigation of size-dependent physicochemical properties of polyamine-functionalized silver nanoclusters. *J. Phys. Chem. C* **2013**, *117*, 3548–3555.
- (48) Manoth, M.; Manzoor, K.; Patra, M.; Pandey, P.; Vadera, S.; Kumar, N. Dendrigraft polymer-based synthesis of silver nanoparticles showing bright blue fluorescence. *Mater. Res. Bull.* **2009**, *44*, 714–717.
- (49) Gupta, A.; Das, R.; Yesilbag Tonga, G.; Mizuhara, T.; Rotello, V. M. Charge-switchable nanozymes for bioorthogonal imaging of biofilm-associated infections. *ACS Nano* **2018**, *12*, 89–94.
- (50) Huo, S.; Jiang, Y.; Gupta, A.; Jiang, Z.; Landis, R. F.; Hou, S.; Liang, X. J.; Rotello, V. M. Fully Zwitterionic Nanoparticle Antimicrobial Agents through Tuning of Core Size and Ligand Structure. *ACS Nano* **2016**, *10*, 8732–8737.